

Hyperfine-controlled domain-wall motion observed in real space and time

John N. Moore,¹ Junichiro Hayakawa,¹ Takaaki Mano,² Takeshi Noda,² and Go Yusa^{1,*}

¹*Department of Physics, Tohoku University, Sendai 980-8578, Japan*

²*National Institute for Materials Science, Tsukuba, Ibaraki 305-0047, Japan*

(Dated: October 18, 2016)

We perform real-space imaging of propagating magnetic domains in the fractional quantum Hall system using spin-sensitive photoluminescence microscopy. The propagation is continuous and proceeds in the direction of the conventional current, i.e. opposite to the electron flow direction. The mechanism of motion is shown to be connected to polarized nuclear spins around the domain walls. The propagation velocity increases when nuclei are depolarized, and decreases when the source-drain current generating this nuclear polarization is increased. We discuss how these phenomena may arise from spin interactions along the domain walls.

PACS numbers: 75.78.Fg, 73.43.-f, 76.60.-k, 42.30.-d

Research around magnetic domains and their dynamics has become increasingly relevant, driven by the hunt for domain-based logic and memory [1, 2]. These technologies could dramatically reduce device heating while increasing speed. A number of scientifically innovative methods for controlling the propagation of ferromagnetic domain walls have recently been pioneered [3–8]. Across these works numerous interaction phenomena have been identified as driving and assisting domain propagation, ranging from spin-transfer torques from injected electrons and optical pulses, to torques and stabilizing influences from Rashba fields and Dzyaloshinskii-Moriya interactions. Apart from these interactions, another potential control parameter relevant to domain motion is hyperfine interaction.

Coupling between conduction electrons and a material's nuclear spin bath has been known since the 1950's to occur via hyperfine interaction [9]. Recently, nuclear magnetic resonance (NMR) studies in semiconductors have attracted renewed interest for their value in research on quantum information processing, especially in quantum confined nanostructures [10–20]. It has been reported that electron-nuclear spin coupling can lead to dynamic nuclear polarization and sometimes can function as a good control parameter to manipulate electron spins [13, 14], or may cause nuclear polarization to act back on the electronic system in complex ways [15–19]. One system in which hyperfine interaction becomes relevant is the fractional quantum Hall (FQH) system [10], where strongly interacting electrons condense into a 2D liquid at fractional values of the Landau level filling factor ν [21]. At certain values of ν and magnetic field B , this system plays host to a phase transition between two degenerate spin resolved many-bodied ground states, i.e. ferromagnetic and non-magnetic states, in which electron spin polarization P is 1 and 0, respectively. Near this phase transition, bringing the system out of equilibrium with a strong source-drain current can excite into existence stripe-shaped domains, which elongate along the Hall electric field (perpendicular to the source-drain cur-

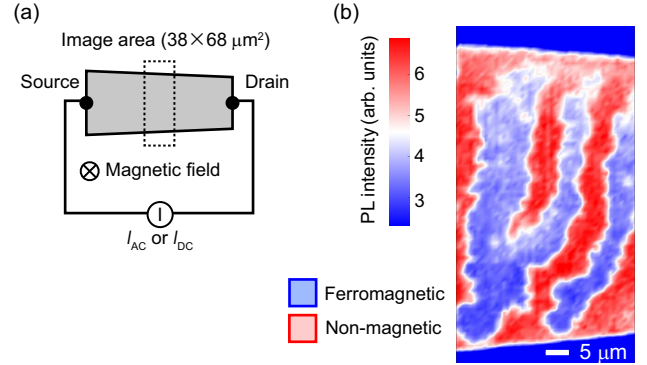


FIG. 1. (Color online) (a) Schematic of the sample. Alternating (I_{AC}) or direct (I_{DC}) current can be applied between the source and drain. External magnetic field B perpendicular to the 2D electrons is 6.8 T throughout. (b) $38 \times 68\text{-}\mu\text{m}^2$ spatial image showing integrated PL intensity of charged exciton singlet peak, at $\nu = 0.666$, with 13-Hz, $I_{AC} = 60$ nA alternating source-drain current. Image step size: 781 nm. $T \sim 60$ mK unless otherwise specified.

rent direction); spin-resolved electrons passing between these domains undergo flip-flop scattering with nuclei, producing nuclear spin polarization P_N near domain walls [22].

In this Letter we investigate the hyperfine-mediated controllability of domain walls in real space and time. Using spin-sensitive photoluminescence (PL) microscopy, we image domains propagating through the sample in response to a direct source-drain current I_{DC} . This propagation is continuous and unidirectional. The propagation velocity increases when nuclei are resonantly depolarized, and it shows dependencies on ν and the magnitude of I_{DC} that also suggest P_N 's tendency to reduce the velocity. We discuss how these phenomena may arise from spin interactions along the domain walls.

Measurements were carried out at temperature $T \sim 60$ mK in a 15-nm-wide GaAs/AlGaAs quantum well sample containing a FQH liquid with ν close to 2/3 and

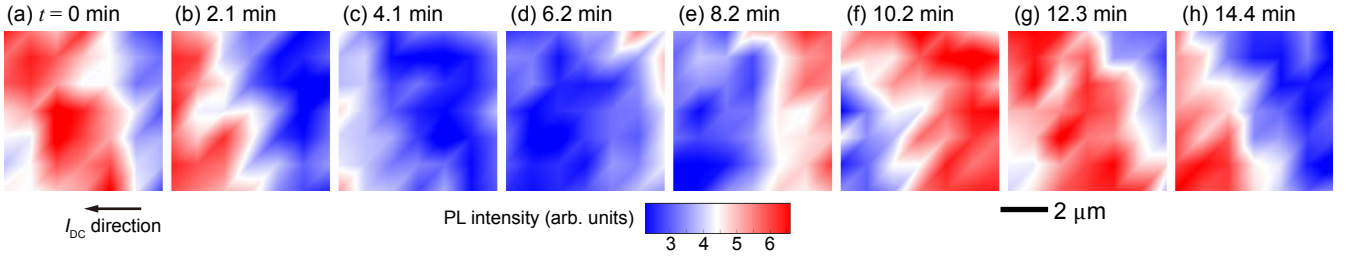


FIG. 2. (Color online) $6 \times 6\text{-}\mu\text{m}^2$ PL-intensity images of the center of the region shown in Fig. 1(b) for t of: (a) 0; (b) 2.1; (c) 4.1; (d) 6.2; (e) 8.2; (f) 10.2; (g) 12.3; and (h) 14.4 min. $I_{\text{DC}} = 110$ nA, $\nu = 0.664$. Image step size: $1\text{ }\mu\text{m}$. See supplementary video [23].

at the critical magnetic field ($B = 6.8$ T) of the $\nu = 2/3$ spin phase transition [24]. An n -doped GaAs substrate functions as a back gate and enables us to tune two-dimensional electron density n_e and ν at constant B . The sample was measured by scanning optical microscopy and spectroscopy. We spatially mapped the integrated PL intensity produced by singlet-state charged excitons [25, 26]; this intensity is primarily anti-correlated with the local P [24], but also is sensitive to the local P_N [22]. Accordingly, the non-magnetic and ferromagnetic domains are distinguished by strong and weak PL intensities, respectively [24]. For comparison to the previous study [22], we applied a 13-Hz *alternating* source-drain current $I_{\text{AC}} = 60$ nA to the sample near the phase transition [Fig. 1(b)]. Upon applying the current, the striped domains that are excited tend to be unstable for the first ~ 1 hr; after this period they appear static over the duration of the imaging (~ 20 hr). The spatial image at $\nu = 0.664$ [Fig. 1(b)] excited by I_{AC} is consistent with that reported earlier showing the formation of domain structures [22].

When, in contrast, a *direct* source-drain current I_{DC} is applied, the scenario is altered dramatically; the domains propagate spatially [Fig. 2(a)–2(h); see SI video]. In Fig. 2(a), a domain wall in the right of the image at an arbitrary time $t = 0$ propagates $3\text{--}4\text{ }\mu\text{m}$ to the left at $t = 4.1$ min [Fig. 2(c)]. Another domain wall propagates across the image in the same manner [Figs. 2(d)–2(g)]. The propagation direction is identical to the current direction, and reversing the current direction reverses the propagation direction. The widths of these striped domains are consistently preserved [23], indicating that the domain walls all have nearly equivalent velocities, possibly because conservation of P throughout the system is energetically favorable.

The integrated microscopic PL (μ -PL) intensity obtained from a diffraction limited spot ($\phi \sim 1\text{ }\mu\text{m}$) at a fixed point under $I_{\text{DC}} = 110$ nA oscillates reasonably periodically in time with a period on the order of ~ 10 min [Fig. 3(a)], suggesting that the stripe domains form with a fairly equally spaced period. In contrast, for $I_{\text{DC}} = 0$ nA, all the imaged area contains a ferro-

magnetic ground state, and the PL intensity at the fixed point is constant over time. The averaged PL intensity for $I_{\text{DC}} = 0$ nA, denoted by a dotted line in Fig. 3(a), is near the center of oscillations observed for $I_{\text{DC}} = 110$ nA. The drops in intensity below this ferromagnetic ground-state value indicate the influence of P_N anti-parallel to B inside of ferromagnetic phase domains. The increases in intensity above the ground-state value are due to the combined influence of P_N parallel to B and the vanishing of P in the non-magnetic phase domains.

In order to obtain the average domain velocity along the horizontal direction v_{domain} , we measured μ -PL intensities at two points (Points 1 and 2) aligned along the length of the Hall bar [Fig. 3(c)]. In this measurement, the μ -PL spectrum was collected for 4 s at Point 1; the measurement position was then immediately shifted $4\text{ }\mu\text{m}$ to the right (Point 2) and the μ -PL spectrum was again collected for 4 s; after returning to the original point (Point 1), the cycle was repeated. A time delay appears in the intensity at these two points due to the domain motion, and its average value can be determined from the cross-correlation between the two sets of oscillations. The cross-correlation is maximum at a time lag of -1.330 min [Fig. 3(d)]. The average velocity of the domains, v_{domain} , at $I_{\text{DC}} = 110$ nA, $\nu = 0.662$, thus, is estimated to be ~ 45 nm/s. The strong cross-correlation confirms that the widths of the striped domains are preserved over short distances on the order of the domain widths.

To investigate the influence of nuclear spins on the domain motion, we depolarized nuclear spins by applying r.f. radiation through a two-turn coil wrapped around the sample. v_{domain} increases when r.f. is applied to resonantly depolarize the ^{75}As nuclei that have been polarized by I_{DC} (Fig. 4). We applied r.f. over a range of powers, both resonantly (red) and off-resonantly (blue). The resonance and off-resonance frequencies were determined from the optically detected NMR spectrum taken in this sample at the same B [22]. There is a velocity difference of $30\text{--}40$ nm/s between the two frequency cases, independent of r.f. power, $P_{\text{r.f.}}$ (Fig. 4), which clearly indicates that polarized nuclear spins hamper domain motion

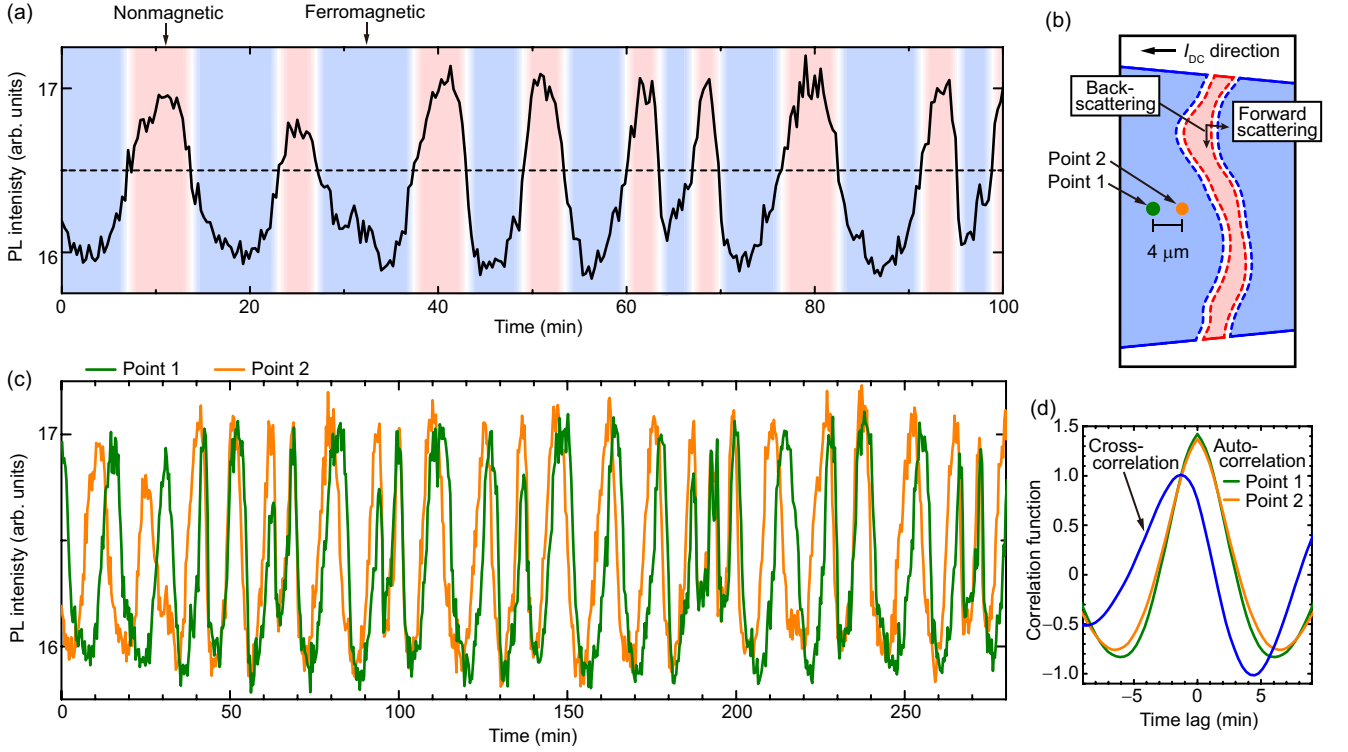


FIG. 3. (Color online) (a) μ -PL intensity at fixed point as function of time with arbitrary $t = 0$, $I_{DC} = 110$ nA; $\nu = 0.662$. Horizontal dotted line corresponds to intensity when $I_{DC} = 0$ nA. (b) Schematic of sample describing locations of Points 1 and 2. Solid and dotted lines denote edge channels and backscattering paths, respectively. (c) μ -PL intensity as function of time at Points 1 (green) and 2 (orange) in the same conditions as Fig. 3(a). (d) Auto-correlation functions of PL intensity at Points 1 (green) and 2 (orange), and cross-correlation function between PL intensity at Points 1 and 2 (blue) as function of time lag.

and that v_{domain} can be increased by *resonantly* decreasing P_N . v_{domain} for both cases increases monotonically with $P_{\text{r.f.}}$. We attribute this increase to the temperature increase (Fig. 4 inset), which also has the tendency to reduce P_N via the thermal energy ($k_B T \sim 5.2$ μ eV for 60 mK, where k_B is Boltzman constant). This energy can *non-resonantly* decrease P_N because of the small Zeeman energy of nuclear spins (~ 0.2 μ eV and ~ 0.4 for ^{75}As and ^{71}Ga , respectively, at $B = 6.8$ T).

v_{domain} is also a function of ν [Fig. 5(a)]. v_{domain} is smallest near the phase transition ($\nu = 2/3$) and is increased by detuning ν away from $2/3$. Given that P_N tends to slow down the propagation, the minimum in v_{domain} seen near to the phase transition is expected because P_N is generated most effectively near the phase transition. I_{DC} also influences v_{domain} [Fig. 5(b)]. The tendency for monotonic decrease in v_{domain} with increasing I_{DC} can be explained by the increase in P_N generated by the current. Later, we will also discuss other possible mechanisms which may account for this behavior.

The low speed of these domains is noteworthy. Under the alternating current condition used for Fig. 1(b), the current direction alternates with a 77-ms period, and the domain propagation length for one half-cycle is order estimated to be $1 \sim 10$ nm. This is negligibly small

compared to the domain size; thus, the images under alternating current here appear static [Fig. 1(b)] [22].

Comparison of v_{domain} to the velocity of the current is important. The velocity of edge current v_{edge} [along the solid blue and red lines in Fig. 3(b)] is order-estimated to be $v_{\text{edge}} \sim \frac{I_{DC}}{en_e \ell_B} \sim 10^5$ m/s, where $n_e \sim 10^{11}$ cm^{-2} , e is the elementary charge, and ℓ_B is the magnetic length. Electrons contributing to I_{DC} must pass as charge current across the domain walls bridging the two sides of the Hall bar, *i.e.* forward scattering at the domain walls. The average velocity v_{forward} of the forward scattering [across the dotted blue and red lines in Fig. 3(b)], *i.e.* the charge current across a domain wall, is roughly $v_{\text{forward}} \sim \frac{\ell_B}{W} v_{\text{edge}} \sim 10^2$ m/s, where W (~ 60 μ m) is the width of the Hall bar, assuming a uniform current distribution over the domain wall [27]. v_{domain} ($\sim 10^{-7}$ m/s) is, therefore, > 9 orders of magnitude slower than the velocity of the charge current ($\sim 10^2$ m/s). This indicates that the domain propagation does not assist in the charge transport of the source-drain current. Also, the propagation direction is opposite to that caused by the spin-torque transfer mechanism. Thus, an alternative interaction must be the cause of the domain wall motion. Spin-torque transfer cannot be ruled out, however, as a possible explanation of the decrease in v_{domain} with in-

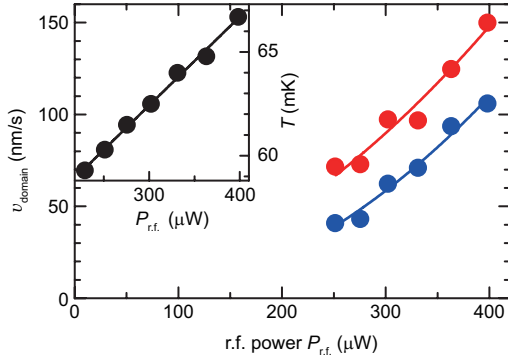


FIG. 4. (Color online) Average domain velocity in I_{DC} direction v_{domain} as function of on-resonant (red, 49.7717 MHz) and off-resonant (blue, 49.84 MHz) r.f. power $P_{\text{r.f.}}$; $I_{DC} = 110$ nA, $\nu = 0.664$. Inset: The dilution refrigerator mixing chamber temperature T as function of $P_{\text{r.f.}}$.

creasing I_{DC} [Fig. 5(b)], as this may reflect spin-torque transfer trying to move the domains in the opposite direction to the observed propagation.

Though we cannot be certain about the specific causes of the domain propagation, we offer here some considerations. One mechanism which might seem to provide an intuitive explanation involves the P_N generated by the current as the driving force [28]. P_N modifies the local electron spin splitting energy [29], and as a result, both magnetic phases become more energetically favorable in the regions along the side of the domain walls where P_N is generated, i.e. the side “downstream” of electron flow. This creates a local perturbation of the domain wall as electrons inside join the favorable phase, displacing the interface. A continued cycle of P_N generation and interface displacement causes an effective motion of the domain walls in the upstream direction, as observed. However, this mechanism of motion is contradicted by the observation of P_N slowing down the domain velocity [Fig. 4].

The domain motion can also be accounted for by steps in the electrochemical potential which are formed by the backscattering channels located along the domain walls. Electronic spin states located on the upper step along each boundary are unstable and may reduce their potential energy by flipping their spins to join the adjacent spin phase. Since no electrons are transported in this process, the domain wall is displaced in the upstream direction. As ν is moved away from the phase transition, states in the domain walls become less stable owing to the larger energy gap between the phases [30], and electron spins may flip more readily, causing v_{domain} to grow away from the transition as observed in Fig. 5(a).

The decrease in v_{domain} with P_N can be accounted for, but it requires a mechanism in which P_N is able to diffuse across the phase boundaries, which is a process that is

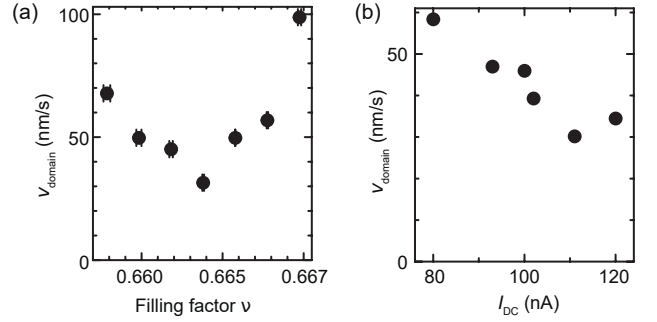


FIG. 5. (a) v_{domain} as function of ν ; $I_{DC} = 110$ nA. Error in ν calculated from uncertainty in electron density. (b) v_{domain} as function of I_{DC} ; $\nu = 0.664$.

thought to be inhibited by electronic spin states making up the domain walls. Because of its direction of polarization, P_N that diffuses across the boundaries acts to decrease the number of nuclei available for electron spin flip-flop exchange processes. Thus, electron spins on the upstream side of domain walls will flip less frequently, and the domain wall motion will be slowed.

The authors are grateful to N. Shibata, K. Muraki, and T. Fujisawa for discussions, and to Y. Hirayama and M. Matsuura for experimental support. This work was supported by the Mitsubishi Foundation and a Grant-in-Aid for Scientific Research (no. 24241039) from the Ministry of Education, Culture, Sports, Science, and Technology (MEXT), Japan. J.N.M. was supported by a Grant-in-Aid from MEXT and the Marubun Research Promotion Foundation. J. H. was supported by a Grant in-Aid from the Tohoku University International Advanced Research and Education Organization.

* yusa@tohoku.ac.jp

- [1] D. A. Allwood, G. Xiong, C. C. Faulkner, D. Atkinson, D. Petit, and R. P. Cowburn, *Science* **309**, 1688 (2005).
- [2] S. S. P. Parkin, M. Hayashi, and L. Thomas, *Science* **320**, 190 (2008).
- [3] M. Yamanouchi, D. Chiba, F. Matsukura, and H. Ohno, *Nature* **428**, 539 (2004).
- [4] A. Yamaguchi, T. Ono, S. Nasu, K. Miyake, K. Mibu and T. Shinjo, *Phys. Rev. Lett.* **92**, 077205 (2004).
- [5] I. M. Miron *et al.*, *Nat. Mater.* **10**, 419 (2011).
- [6] S. Emori, U. Bauer, S.-M. Ahn, E. Martinez and G. S. D. Beach, *Nat. Mater.* **12**, 611 (2013).
- [7] J. H. Franken, M. Herps, H. J. M. Swagten, and B. Koopmans, *Sci. Rep.* **4**, 5248 (2014).
- [8] A. J. Ramsay, P. E. Roy, J. A. Haigh, R. M. Otxoa, A. C. Irvine, T. Janda, R. P. Campion, B. L. Gallagher and J. Wunderlich, *Phys. Rev. Lett.* **114**, 067202 (2015).
- [9] G. Feher, *Phys. Rev. Lett.* **3**, 135 (1959).
- [10] S. Kronmüller, W. Dietsche, K. von Klitzing, G. Denninger, W. Wegscheider, and M. Bichler, *Phys. Rev. Lett.*

- 82**, 4070 (1999).
- [11] T. Machida, T. Yamazaki, K. Ikushima, and S. Komiyama, Appl. Phys. Lett. **82**, 409 (2003).
 - [12] G. Yusa, K. Muraki, K. Takashina, K. Hashimoto, and Y. Hirayama, Nature **434**, 1001 (2005).
 - [13] J. R. Petta, A. C. Johnson, J. M. Taylor, E. A. Laird, A. Yacoby, M. D. Lukin, C. M. Marcus, M. P. Hanson, and A. C. Gossard, Science **309**, 2180 (2005).
 - [14] F. H. L. Koppens, J. A. Folk, J. M. Elzerman, R. Hanson, L. H. Willems van Beveren, I. T. Vink, H. P. Tranitz, W. Wegscheider, L. P. Kouwenhoven, and L. M. K. Vandersypen, Science **309**, 1346 (2005).
 - [15] K. Ono and S. Tarucha, Phys. Rev. Lett. **92**, 256803 (2004).
 - [16] G. Yusa, K. Hashimoto, K. Muraki, T. Saku, and Y. Hirayama, Phys. Rev. B **69**, 161302(R) (2004).
 - [17] C. Latta *et al.*, Nat. Phys. **5**, 758 (2009).
 - [18] I. T. Vink, K. C. Nowack, F. H. L. Koppens, J. Danon, Y. V. Nazarov, and L. M. K. Vandersypen, Nat. Phys. **5**, 764 (2009).
 - [19] S. Hennel *et al.*, Phys. Rev. Lett. **116**, 136804 (2016).
 - [20] H. Sanada, Y. Kondo, S. Matsuzaka, K. Morita, C. Y. Hu, Y. Ohno, and H. Ohno, Phys. Rev. Lett. **96**, 067602 (2006).
 - [21] D. C. Tsui, H. L. Stormer, and A. C. Gossard, Phys. Rev. Lett. **48**, 1559 (1982).
 - [22] J. N. Moore, J. Hayakawa, T. Mano, T. Noda, and G. Yusa, arXiv:cond-mat <http://arxiv.org/abs/1606.06416> (2016).
 - [23] See Supplemental Video on domain propagation in 6×6 - μm^2 PL-intensity images from an arbitrary time $\tau = 0$ to 204 min. $I_{\text{DC}} = 110$ nA, $\nu = 0.664$. Image step size: $1 \mu\text{m}$. Some of the frames of this video are displayed in Fig. 2.
 - [24] J. Hayakawa, K. Muraki, and G. Yusa, Nat. Nano. **8**, 31 (2013).
 - [25] G. Yusa, H. Shtrikman, and I. Bar-Joseph, Phys. Rev. Lett. **87**, 216402 (2001).
 - [26] A. Wójs, A. Gładysiewicz, and J. J. Quinn, Phys. Rev. B **73**, 235338 (2006).
 - [27] v_{edge} is the velocity through a cross-section $\sim \ell_B$, whereas v_{forward} is the velocity through the cross-section $\sim W$. Thus, v_{forward} is $\frac{\ell_B}{W}$ times smaller than v_{edge} , because of the charge conservation law.
 - [28] Flip-flop scattering produces P_N pointing downward (upward) with respect to B after electrons participating in the direct current cross domain walls and join the ferromagnetic (non-magnetic) phase.
 - [29] $E_S = |g^*| \mu_B B - A \langle I_z \rangle$, where g^* is the effective g -factor of electrons, μ_B is the Bohr magneton, $A > 0$ is the hyperfine constant, and $\langle I_z \rangle$ is the average of the nuclear spin quantum number.
 - [30] N. Shibata and K. Nomura, Phys. Soc. Jpn. **76**, 103711 (2007).